Radioactivity Concentration Index Evaluation of Construction Materials by Gamma-ray Spectroscopy

Jin-Goo Kang [a], Soobin Lim [a], Kyoung-Jae Chung [a], Geehyun Kim [a*]
[a]*Department of Nuclear Engineering, Seoul National Univ., Seoul, South Korea*
[*]*Corresponding author: gk.rs@snu.ac.kr*

1. Introduction

Natural occurring radioactive material (NORM) contains potassium (^{40}K), long-lived uranium (^{238}U) and thorium (^{232}Th). ^{238}U and ^{232}Th follow radioactive decay chain respectively producing radon (^{222}Rn) and thoron (^{220}Rn) until reaching a stable isotope (^{206}Pb and ^{208}Pb). Inhalation of radon (^{222}Rn) accounts for more than 50% of annual effective radiation dose [1]. To manage radon concentration of building materials, "guidelines for reduction and management of radon in building materials" apply radioactivity concentration index to building materials [2]. Non-destructive γ-ray spectroscopy is effective method to assess radioactivity concentration without structural change of building materials and compare the amount of radon exhalation from building materials with radioactivity concentration index.

2. Methods and Results

Measurement system is set up to assess radioactivity of construction sample using High Purity Germanium (HPGe) detector. Measurement of activity concentration of concrete is conducted, primary radon-emitting building material, which is supplied from LH (Korea Land & Housing Cooperation). Calibration of the detector is conducted using both experiments and Monte Carlo simulation (MCNP6). Finally, radioactivity concentration index is obtained.

2.1 Measurement System

Shielding background radiation is essential for measurement of radioactivity, as building materials are made of NORM resulting in containing low activity of radionuclides. High Purity Germanium (HPGe) detector measure radioactivity of the sample under background radiation shielded circumstances consisting of lead bricks and 1 cm thickness copper box (Fig. 1).

The level of background radiation was measured for 24 hours and significantly reduced, making possible to detect γ-ray peaks having low counts (Fig. 2). Minimum detectable activity (MDA) of ^{40}K is calculated using equations (1), (2):

$$MDA = \frac{N_D}{\eta \varepsilon_{abs} T} \quad (1)\ [3]$$

$$N_D = 2.706 + 4.653\sigma_B \quad (2)$$

where η is branching ratio of γ energy, $\boldsymbol{\varepsilon}_{abs}$ is absolute peak efficiency, T is measurement time and N_D is minimum mean number of counts needed from the source ensure a false-negative rate no longer than 5% (Eq. 1). And σ_B is standard deviation of background counts (Eq. 2). MDA is decreased by more than half from 59.389 to 24.851 Bq in the system.

Fig. 1. Schematic view (left) and configurations (right) of measurement system consisting of HPGe detector, LN_2 dewar, lead bricks and 1 cm thickness copper box.

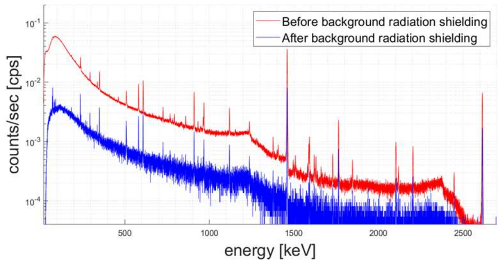

Fig. 2. Effects of shielding systems on the background radiation spectra.

2.2 Energy Calibration

Energy calibration of the detector system is conducted using γ standard sources of ^{241}Am, ^{133}Ba, ^{109}Cd, ^{57}Co, ^{60}Co, ^{137}Cs, ^{152}Eu, ^{54}Mn, ^{22}Na covering energy range from 59.5 keV to 1408.0 keV. Energy calibration curve is determined as equation (3) with $R^2 = 0.9999$:

$$Energy = 0.181 \times Channel + 1.433 \quad (3)$$

2.3 Efficiency Calibration

Efficiency calibration of the detector system is conducted using the standard sources and MCNP6 simulations. After γ-ray standard sources are measured respectively, net area of peak is calculated. ROI of peak area is set from -1.6×FWHM to 1.4×FWHM from the peak centroid, calculated from gaussian fitting of full energy peak. Intrinsic peak efficiency is calculated using equation (4):

$$\varepsilon_{int} = \frac{N_{net}}{A \cdot \eta \cdot \frac{\Omega}{4\pi} \cdot T} \quad (4)$$

where A is activity, and Ω is solid angle. Intrinsic peak efficiency is determined from 59.5 keV to 1408.0 keV (Fig. 3).

To consider self-attenuation of γ-ray, dead layer of HPGe crystal is corrected, verifying between experiment results and simulation (Fig. 3). Dead layer of the crystal is determined to 1.23 mm. Finally, absolute peak efficiency considered for solid angle and self-attenuation is derived through MCNP6 simulation (Fig. 4).

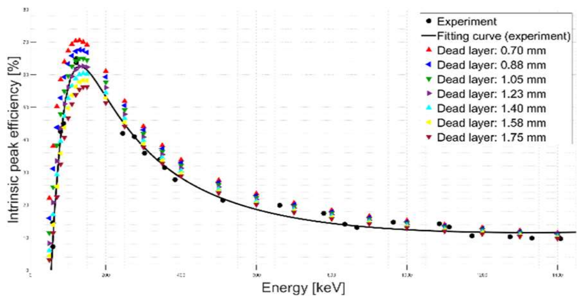

Fig. 3. Intrinsic peak efficiency calibration of the detector by adjusting dead layer about MCNP6 simulation and experimental results of γ-ray standards.

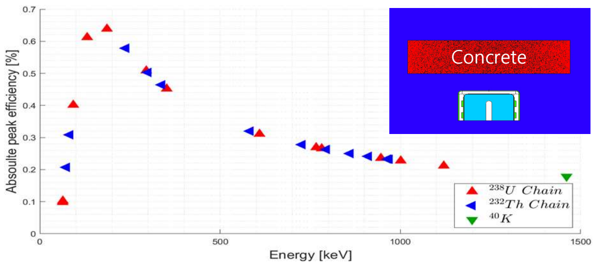

Fig. 4. Absolute peak efficiency results of the detector and concrete configurations (size: $20 \times 20 \times 5\ cm^3$).

2.4 Radioactivity Concentration Index (I)

Radioactivity concentration index guided in Korea is calculated using equations (5), (6):

$$I = \frac{A_{^{226}Ra}}{300} + \frac{A_{^{232}Th}}{200} + \frac{A_{^{40}K}}{3000} \quad (5)\ [2]$$

$$A_x = \frac{N_{net}}{\eta \cdot \varepsilon_{int} \cdot T \cdot m}\ (Bq \cdot kg^{-1}) \quad (6)$$

where A_x is activity concentration, N_{net} is net area, and m is mass of measured sample.

For ^{226}Ra and ^{232}Th, in addition to directly determining the concentration of the nuclide, the concentration was obtained indirectly by analyzing radionuclides in decay chains, using the fact that the nuclides of the decay chain follow radiative equilibrium. Overlapped photopeak at ~186 keV is corrected by determining ^{235}U concentration from both 143.8 keV γ-ray of ^{235}U and natural abundance of ^{238}U concentration [4]. Likewise, overlapped photopeak at ~63.5 keV is corrected by determining ^{232}Th concentration from activity concentration of ^{228}Ac.

^{226}Ra and ^{232}Th range respectively from 56.3 to 70.8 and from 42.6 to 61.0 Bq·kg^{-1}. And the concentration of ^{40}K is 834.8 Bq·kg^{-1}. Activity concentration index (I) for concrete sample ranges from 0.682 ± 0.020 to 0.819 ± 0.028. Activity concentration index of ^{226}Ra, ^{232}Th and ^{40}K accounts for 28.7%, 34.0% and 37.1%. (Table I)

Table I: Radioactivity Concentration Index about Radionuclide in Concrete sample (size: $20 \times 20 \times 5\ cm^3$)

Radionuclide	Decay Chain	Energy (keV)	Branching Ratio (%)	Concentration (Bq/kg)	Activity Concentration Index (I)		
^{226}Ra	^{238}U	**186.2**	3.56	56.3 ± 4.0	0.188 ± 0.013	**0.188 – 0.236**	**0.682 – 0.819**
^{234}Th		**63.3**	3.75	70.8 ± 8.5	0.236 ± 0.028		
^{232}Th	^{232}Th	**63.8**	0.26	51.1 ± 2.6	0.256 ± 0.013	**0.213 – 0.305**	
^{228}Ac		**270.2**	3.55	50.9 ± 2.7	0.254 ± 0.014		
		328.0	3.04	42.6 ± 2.9	0.213 ± 0.015		
		338.3	11.40	48.6 ± 0.9	0.243 ± 0.005		
		409.5	2.02	55.7 ± 4.2	0.278 ± 0.021		
		463.0	4.45	51.8 ± 2.0	0.259 ± 0.010		
		794.5	4.25	45.3 ± 2.4	0.226 ± 0.012		
		835.7	1.70	61.0 ± 5.0	0.305 ± 0.025		
		911.2	26.20	49.8 ± 0.7	0.249 ± 0.003		
		964.8	4.99	55.1 ± 2.1	0.275 ± 0.011		
		969.0	15.90	50.5 ± 0.9	0.253 ± 0.005		
^{40}K	-	**1460.8**	10.55	834.8 ± 4.2	0.278 ± 0.001	**0.278**	
^{235}U	^{235}U	**143.8**	10.94	1.8 ± 0.8	-	-	-
		185.7	57.00	-	-	-	-

3. Conclusions

Non-destructive γ-ray spectroscopy is conducted for building material. To minimize the effect of the background radiation, measurement system is set up. Calibration is performed to measure bulk sample considering self-attenuation effect. The index of radioactivity concentration is determined both directly and indirectly using radiative equilibrium. Obtained index is less than 1, which is the recommended limit in the guideline. As inhalation of radon closely related to concentration of ^{226}Ra, the level of ^{220}Rn exhalation should be compared with radioactivity concentration index in the future.

ACKNOWLEDGEMENTS

This research was supported by the Korea Land and Housing Corporation (LH).

REFERENCES

[1] L. Fior, J. Nicolosi Corrêa, S.A. Paschuk, V.V. Denyak, H.R. Schelin, B.R. Soreanu Pecequilo, J. Kappke, Activity measurements of radon from construction materials, Applied Radiation and Isotopes, Vol. 70, Issue 7, pp.1407-1410, 2012.

[2] Ministry of Environment, Ministry of Land, Infrastructure and Transport, Nuclear Safety and Security Commission, "Guidelines for Reduction and Management of Radon in Building Materials", p.2, Nov. 2019.

[3] G. F. Knoll, Radiation Detection and Measurement, John Wiley & Sons, New York, pp.95-98, 2010.

[4] N.P. Petropoulos, M.J. Anagnostakis, S.E. Simopoulos, Photon attenuation, natural radioactivity content and radon exhalation rate of building materials, Journal of Environmental Radioactivity, Vol. 61, Issue 3, pp.257-269, 2002.